Time-Dependent Taylor Vortices in Wide-Gap Spherical Couette Flow

Rainer Hollerbach*

Department of Mathematics, University of Glasgow, Glasgow G12 8QW, United Kingdom

(Received 17 June 1998)

Motivated by recent experimental work, I numerically investigated the possibility of obtaining Taylor vortices in a spherical shell of aspect ratio 0.336. It is found that Taylor vortices can exist for Reynolds numbers in the range $415 \leq \mathrm{Re} \leq 2040$. With increasing Reynolds number, the initially equatorially symmetric vortices become asymmetric at $\mathrm{Re} = 1390$. Increasing Re still further, these asymmetric vortices become time dependent at $\mathrm{Re} = 1940$, followed by a period-doubling cascade to chaos at $\mathrm{Re} \approx 2035$. For $\mathrm{Re} > 2040$ the chaotic solution collapses back to the basic state having no Taylor vortices. [S0031-9007(98)07310-4]

PACS numbers: 47.32.Cc, 47.20.Ky

Spherical Couette flow is the flow induced in a fluid-filled spherical shell by fixing the outer sphere and rotating the inner one. Couette flows—in cylindrical [1] as well as spherical geometry—are among the most fundamental problems in classical fluid dynamics, and the study of these flows has contributed enormously to our understanding of hydrodynamic instabilities of many different kinds, with the interplay between experimental, numerical, and analytical work being particularly important. This Letter represents one such comparison between experimental and numerical work. The numerical results presented here not only help to explain previous experimental results [2], they also suggest further experiments to look specifically for some of the novel features described here.

We start with the Navier-Stokes equation,

$$\frac{\partial}{\partial t}\mathbf{U} + \mathbf{U}\cdot\nabla\mathbf{U} = -\nabla p + \nu\nabla^2\mathbf{U}\,,$$

together with the incompressibility condition $\nabla\cdot\mathbf{U} = 0$ and the boundary conditions

$$\mathbf{U} = \Omega r\sin\theta\,\hat{\mathbf{e}}_\phi \quad \text{at } r = r_i\,,$$
$$\mathbf{U} = 0 \quad \text{at } r = r_o\,,$$

where Ω is the prescribed rotation rate of the inner sphere. Spherical Couette flow is thus governed by two parameters: the aspect ratio $\beta \equiv (r_o - r_i)/r_i$ measuring the basic geometry, and the Reynolds number $\mathrm{Re} \equiv r_i^2\Omega/\nu$ measuring the forcing. In a typical experiment one fixes the aspect ratio and scans through a range of Reynolds numbers to determine the possible flow states. On the basis of numerous experiments [3–7] it was believed that $\beta \approx 0.24$ constituted a boundary between two distinct dynamical regimes, with purely axisymmetric Taylor vortices occurring only for $\beta < 0.24$. In contrast, for $\beta > 0.24$ it was found that the first instability was directly to a fully three-dimensional flow [5,6,8]. As a result, most previous experimental [4,7,9] as well as numerical [9–12] work has focused on the $\beta < 0.24$ regime, and relatively little on the $\beta > 0.24$ regime.

However, by using some special initial conditions in which the outer sphere is temporarily also rotated, Liu *et al.* [2] were able to generate Taylor vortices in a shell of aspect ratio 0.336. They write that "Taylor vortices coexist in the range of about $470 \leq \mathrm{Re} \leq 2100$ and merge into the basic flow state at both Re limits." One purpose of this work then is simply to determine the precise mechanism whereby these vortices merge back into the basic state at the two limits, and indeed we will discover that two quite different bifurcations are involved. Another aspect of these experiments requiring explanation is that for sufficiently large Reynolds numbers they observed equatorially asymmetric Taylor vortices, and yet when they attempted to reproduce this phenomenon numerically, they only ever found symmetric vortices. In this work we certainly find asymmetric vortices as well, and offer one plausible explanation as to why Liu *et al.* did not.

The time-stepping pseudospectral code [13] used in this work was originally developed with various geophysical and astrophysical magnetoconvection problems in mind, but has been benchmarked against the spherical Couette flow problem by reproducing some of the results of Mamun and Tuckerman [12] at $\beta = 0.154$, with excellent agreement in every case tried. The typical truncation used was 25 Chebyshev modes in r times 160 spherical harmonic modes in θ, with a few runs also done at higher truncations to verify that 25×160 is sufficient to resolve the flow structures even at the highest Reynolds numbers.

Not surprisingly, starting the code off with zero initial conditions and time stepping until one reaches a steady state yields only the basic state having no Taylor vortices. Figure 1(a) shows the meridional circulation at $\mathrm{Re} = 420$, which one notes consists simply of one circulation cell in each hemisphere, with outflow at the equator and inflow at the poles. (Even though the flow is forced by the imposed rotation of the inner sphere, it is preferable to show the meridional circulation rather than the azimuthal velocity, as it is in the meridional circulation that the Taylor vortices manifest themselves.)

In order to obtain Taylor vortices, one thus has to start off with different initial conditions. Rather than attempt to follow the experimental procedure [2], which involves fully three-dimensional intermediate stages, it

 0031-9007/98/81(15)/3132(4)$15.00

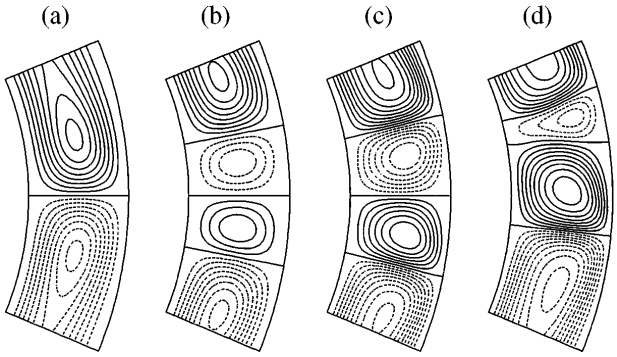

FIG. 1. Streamlines of the meridional circulation, with counterclockwise flow shown as solid lines, clockwise flow as dashed lines. To focus attention on the most interesting aspects, only the equatorial region $3\pi/8 \le \theta \le 5\pi/8$ is shown; in each case the truncated circulation cells close in the polar regions. From left to right: (a) The basic state at Re = 420; (b) and (c) the Taylor vortex state at Re = 420 and 1380, respectively; and (d) the asymmetric Taylor vortex state at Re = 1900.

proved easiest first to obtain a Taylor vortex state at a smaller aspect ratio. For $\beta = 0.154$ it is known [12] that for certain Reynolds numbers the desired state is the only stable state, and so one will inevitably reach it. Then one simply gradually increases β until one has the corresponding state at $\beta = 0.336$. (The ability to adjust β continuously is one clear advantage of numerics over experiments in this area.) Figure 1(b) shows this state, again at Re = 420, and one notes very clearly the pair of Taylor vortices straddling the equator.

Having found the Taylor vortex state, one wants to track its evolution with varying Reynolds number. At the lower limit one discovers that it simply ceases to exist below Re = 415, almost certainly as a result of a saddle-node bifurcation, just as for $\beta = 0.154$ [12]. That the experimentally determined lower limit of 470 is somewhat greater presumably indicates that this state is already becoming increasingly vulnerable to small perturbations as one approaches the turning point. At the upper limit, one can increase Re by more than a factor of 3 without discovering any further bifurcations; Fig. 1(c) shows the Taylor vortex state at Re = 1380, and one notes that the vortices are more strongly developed than in Fig. 1(b), but otherwise the two are clearly the same state.

The next bifurcation occurs at Re = 1390, in the form of a supercritical pitchfork bifurcation to an equatorially asymmetric state. Figure 1(d) shows this state at Re = 1900, by which point the asymmetry is quite pronounced. It would seem that we have thus succeeded in obtaining the asymmetric vortices of Liu *et al.* [2]. There is one slight difficulty, though, namely, that according to Liu *et al.*, "The asymmetry appears in most cases already at Re $\approx$ 650, but in some cases at Re $\approx$ 1100 first." Having an asymmetry that sometimes appears at one Reynolds number and sometimes at another is already puzzling enough, but that neither of these values should agree with the numerically predicted value is downright disconcerting. However, if one examines Fig. 4(b) of Liu *et al.*, one finds that the observed asymmetry is relatively slight until Re $\approx$ 1300–1400, at which point it suddenly increases quite substantially. I would thus argue that the bifurcation to a genuinely asymmetric state is indeed occurring at Re = 1390, and that the asymmetry they observed before then is simply the inevitable asymmetry associated with the lack of perfect equatorial symmetry in their apparatus. This would certainly also explain why they did not succeed in obtaining this asymmetric state numerically; they were simply looking in the wrong range of Reynolds numbers. (And in the high Re range where we have shown that the asymmetric state does exist, their truncation of 25 $\times$ 120 finite-difference grid points almost certainly would not have been sufficient.)

Having obtained the asymmetric state, and having argued that it is, in fact, in good agreement with the experiments, we continue increasing Re. Quite unexpectedly, a supercritical Hopf bifurcation occurs at Re = 1940—unexpected because Liu *et al.* made no mention of any time dependence in their results. Figure 2 shows one period of this state at Re = 2000, and one notes that the time dependence consists of a fluctuation in the strength of the smaller of the two Taylor vortices. However, by looking at Fig. 2 one also begins to understand why Liu *et al.* did not notice any time dependence; the flow at either boundary—experimentally the most readily observable part—is indeed almost constant. More quantitatively, if one considers the torque one must exert on the inner sphere to maintain its constant rotation, one finds that it only varies by 0.5% throughout the period of $28.6\Omega^{-1}$. Nevertheless, by knowing at precisely what frequency to look, it might be possible to observe even such a small fluctuation experimentally. Finally, one might just note that, as small as its fluctuations are, this time-dependent state is the first time a stable Hopf bifurcation has been discovered in purely axisymmetric spherical Couette flow (although such bifurcations are known to exist in cylindrical Couette flow [14,15]).

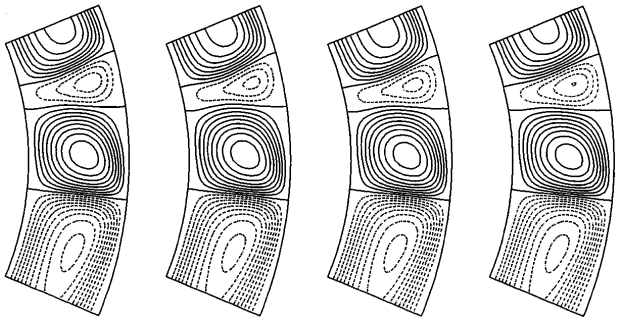

FIG. 2. The meridional circulation of the time-dependent state at Re = 2000. From left to right are four snapshots uniformly spaced throughout the period of $28.6\Omega^{-1}$.

The next bifurcation is a period doubling at Re = 2010. Figure 3 shows one period of this state at Re = 2025. One notices first of all that these fluctuations in the strength of the small Taylor vortex have increased, with the maximum being greater and—what will ultimately turn out to be more important—the minimum being smaller. (Correspondingly, the torque now varies by 0.8% throughout the period.) One notices also that the period doubling consists of the original cycles being alternately more (top row) and less (bottom row) pronounced. Further increasing Re, another period doubling occurs at Re = 2030, with Fig. 4 showing one period of this state. One notes that these fluctuations in the strength of the small Taylor vortex have increased some more, and that the period doubling consists of a further modulation of the original cycles. Finally, by Re = 2035 one has what appears to be a chaotic state, with the strength of the Taylor vortex fluctuating in an irregular manner. It would thus appear that these two period doublings are merely the first two in a cascade to chaos [16]. (While it would be nice to find a few more doublings, and hence verify that this is indeed the route to chaos, that is unfortunately hardly feasible in a dynamical system having $2 \times 25 \times 160 = 8000$ degrees of freedom.)

The last thing we would like to understand is why this chaotic state collapses back to the basic state having no Taylor vortices once Re exceeds 2040. We already know that the general character of all of these time-dependent solutions consists of a fluctuation in the strength of the smaller of the two Taylor vortices, regular in the periodic regime, irregular in the chaotic regime. We have also seen how these fluctuations become increasingly large for increasingly large Re. It is thus plausible that the collapse back to the basic state is caused by the fluctuations somehow becoming too large. If one starts with an equilibrated solution at Re = 2040 and suddenly increases it to 2045, for several dozen fluctuation cycles nothing seems to happen (with the precise duration of these chaotic transients obviously depending on the precise starting solution). However, Fig. 5 shows what happens then. In the first frame in Fig. 5 the solution still looks much like before, except that this small Taylor vortex is weaker than anything we have seen before. Indeed, it is now so weak that it cannot recover to carry on as before; instead it disappears entirely. At the same time the large Taylor vortex reconnects with the upper circulation cell. Once both Taylor vortices are thus destroyed, the resulting solution quickly relaxes back to the symmetric basic state having no vortices—not surprisingly, since it is known that this state is stable throughout the entire range of Reynolds numbers considered here. From a fluid-dynamical point of view this collapse is thus caused by the instability of a very small vortex sandwiched between two large and oppositely directed ones. From a dynamical-systems point of view it is caused by the gradual expansion of the chaotic solution to

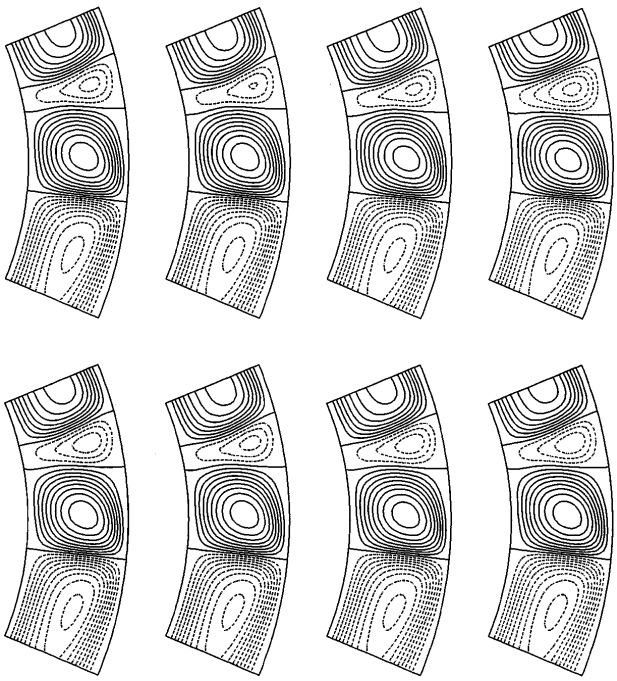

FIG. 3. The meridional circulation of the time-dependent state at Re = 2025. From top left to bottom right are eight snapshots uniformly spaced throughout the period of $55.2\Omega^{-1}$. Each row thus corresponds to one of the fluctuation cycles previously seen in Fig. 2, and the difference between the two shows the effect of the first period doubling.

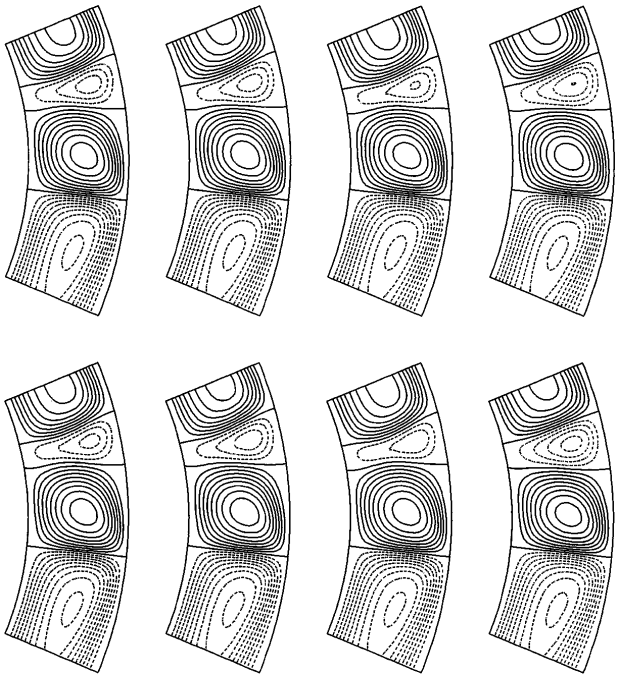

FIG. 4. The meridional circulation of the time-dependent state at Re = 2030. From top left to bottom right are eight snapshots uniformly spaced throughout the period of $109.3\Omega^{-1}$. The difference between the two rows thus shows the effect of the second period doubling (and within each row the difference between the first and second two frames once again shows the effect of the first period doubling).

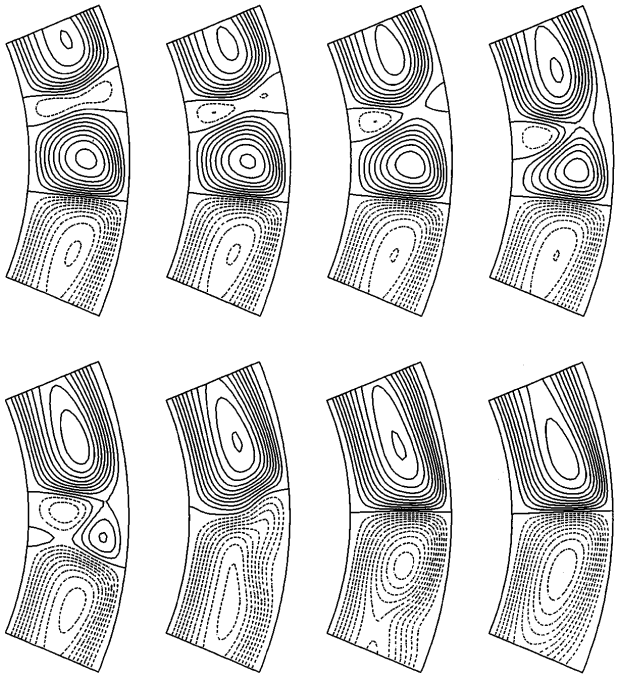

FIG. 5. The final collapse at Re = 2045. From top left to bottom right are eight uniformly spaced snapshots covering a total time of $16\Omega^{-1}$.

where it reaches the basin of attraction of another solution. A bifurcation of this type is known as a boundary crisis [17] or also as a chaotic blue sky catastrophe [16].

To summarize, in this work we have considered the possibility of obtaining Taylor vortices in a spherical shell of aspect ratio 0.336. We have shown that Taylor vortices can exist in the range $415 \leq \mathrm{Re} \leq 2040$, terminating in a saddle-node bifurcation at the lower end, and in a boundary crisis at the upper end. These results are in generally good agreement with the experimentally [2] determined range $470 \leq \mathrm{Re} \leq 2100$. We have shown that the Taylor vortices become asymmetric at Re = 1390, and have argued that this is, in fact, also in good agreement with the experimental results. We also discovered that the vortices become time dependent at Re = 1940, and showed how this time dependence is crucial in understanding the nature of the final collapse beyond Re = 2040. Although this time dependence was not observed experimentally, we have suggested why, and have suggested further experiments now that it is known what to look for.

Finally, from the point of view of further numerics one could do, one might just note that the bifurcation sequence we have described here for $\beta = 0.336$ is very different from the sequence described by Mamun and Tuckerman [12] for $\beta = 0.154$. For example, here we found a stable Hopf bifurcation, whereas they found an unstable one. Indeed, given all the other differences between the two bifurcation diagrams, it is not even clear that these two Hopf bifurcations would merge into one another as one varies β. It would thus be of interest to map out the bifurcation diagram not just for fixed β and varying Re, but for varying β as well. Mapping out such a two-parameter bifurcation diagram in a dynamical system having 8000 degrees of freedom will be a formidable undertaking though.

I thank Eun-jin Kim for a valuable and enjoyable discussion of this problem and its various bifurcations; I thank Paul Fotheringham for his assistance with the graphics. This work was supported by the Nuffield Foundation.

*Electronic address: rainer@maths.gla.ac.uk

[1] G. I. Taylor, Philos. Trans. R. Soc. London A **223**, 289 (1923).
[2] M. Liu, C. Blohm, C. Egbers, P. Wulf, and H. J. Rath, Phys. Rev. Lett. **77**, 286 (1996).
[3] G. N. Khlebutin, Fluid Dynam. **3**, 31 (1968).
[4] O. Sawatzki and J. Zierep, Acta Mech. **9**, 13 (1970).
[5] B. R. Munson and M. Menguturk, J. Fluid Mech. **69**, 705 (1975).
[6] I. M. Yavorskaya, Yu. N. Belyaev, and A. A. Monakov, Fluid Mech. **5**, 660 (1975).
[7] M. Wimmer, J. Fluid Mech. **78**, 317 (1976); **103**, 117 (1981).
[8] C. Egbers and H. J. Rath, Acta Mech. **111**, 125 (1995).
[9] K. Bühler, Acta Mech. **81**, 3 (1990).
[10] F. Bartels, J. Fluid Mech. **119**, 1 (1982).
[11] P. S. Markus and L. S. Tuckerman, J. Fluid Mech. **185**, 1 (1987).
[12] C. K. Mamun and L. S. Tuckerman, Phys. Fluids **7**, 80 (1995).
[13] R. Hollerbach (to be published).
[14] T. Mullin, K. A. Cliffe, and G. Pfister, Phys. Rev. Lett. **58**, 2212 (1987).
[15] S. J. Tavener, T. Mullin, and K. A. Cliffe, J. Fluid Mech. **229**, 483 (1991).
[16] J. M. T. Thompson and H. B. Stewart, *Nonlinear Dynamics and Chaos* (Wiley, Chichester, 1986).
[17] C. Grebogi, E. Ott, and J. A. Yorke, Phys. Rev. Lett. **48**, 1507 (1982); Physica (Amsterdam) **7D**, 181 (1983).